Tool Wear Analysis and Process Parameter Optimization for Variable Curvature Machining of Aircraft Blades

Ting Chen[1], Lei Li[1], Yun Xu[1, *], Jiahu Zhang[1], Qi Li[2]

[1] School of Mechanical Engineering, Sichuan University of Science and Engineering, Zigong 643000, China

[2] SICHUAN CHANGZHENG MACHINE TOOL GROUP co,LTD, Zigong 643000, China

Abstract

In this paper, due to the improper selection of process parameters in curved surface milling, the tool wear is accelerated, and the surface quality and dimensional accuracy of parts are difficult to control. Using BBD orthogonal test and extreme difference analysis method, based on the basic theory of thermo-mechanical coupling elastic-plastic mechanics, the application of Deform-3D finite element simulation software to complete the simulation of blade milling machining simulation can be obtained tool wear and the rule of change of milling temperature. Analysis of variance was used to test the degree of fit between the mathematical model and test value (P<0.0001). Taking tool wear and material removal rate as optimization objectives and spindle speed, feed per tooth, and milling depth as constraints, a multivariate quadratic regression model of process parameters was established. The optimum combination of process parameters was obtained by the multi-objective optimization method. The results show that, without considering other conditions, effective machining parameters combination can be obtained through the multi-objective optimization method, achieving control tool wear and improving material removal rate.

Keywords

Navigation Hair Blades; Finish Machining; Tool Wear Rate; Material Removal Rate; Multi-objective Optimization Algorithm.

1. Introduction

Aero-engine blade surfaces change all the time during the machining process, The Contour change rate required <0.008mm[1], If the process parameters are not selected properly, it will accelerate tool wear and seriously affect the quality of blade machining. To ensure the quality of blade processing in actual production, conservative empirical process parameters are often used, resulting in low efficiency and high cost of titanium alloy parts processing. Therefore, it is crucial to study the control methods of tool wear and material removal rate to improve the blade machining accuracy.

To control the process parameters to reduce tool wear rate and improve machining efficiency at home and abroad scholars have carried out a lot of research. Zheng Minli [2] and others established a milling force prediction model based on machining characteristics for the milling process of internal and external corners of mold cavities. Wang Xiaochun [3] and others study the effect of tool path curvature on milling force during side milling of small diameter milling cutters. Yang Torch [4] studied in depth the cutting temperature and tool wear for machining complex surfaces of titanium alloys. Liang, Xiaoliang [5] A study on the law of influence of tool wear state on the surface integrity of machined titanium alloy Ti-6Al-4V. Liu [6] et al. investigated the analysis of the effect of variable curvature surface geometric features on machining errors. Senthil Kumara [7] et al. derived an

empirical formula for tool wear by fitting a multivariate linear regression through a three-stage representation of the worn form of the approximate curve. Effect of front and back angles on tool life. Jawahir I s et al [8] considered the effect of cutting conditions and workpiece hardness on tool wear in their tool life prediction model.

The above study provides methods for tool wear control and parameter optimization, Most researchers are still targeting special bevels and fixed process parameters. There are fewer studies on ball-end milling cutters for milling free-form profile finishing under variable operating conditions.

In this paper, the radius of curvature of the blade profile is utilized for the study, and DEFORM-3D performs finite element simulation on the blade profile to obtain the relationship between the process parameters in a certain range of tool temperature and the amount of tool wear, Mathematical modeling of tool wear, material removal rate and process parameters, With the objectives of relatively low tool wear and relatively high material removal rate, a multi-objective optimization algorithm is used to obtain the Pareto optimal solution set to obtain the preferred process parameter set.

2. Multi-axis High-speed Milling Cutter-work Contact Area Modeling

(1) Tool-workpiece contact arc segment extraction

The process of milling blades with ball end milling cutters is very complicated due to the complexity and distortion of the blade profile. Need to use a 5-axis mill-turn machine or a 5-axis blade machining machine for molding and precision control. Automatic planning of the tool path during blade surface milling is more difficult, and the position of the milling point on the tool is constantly changing, as shown in 1.

Figure 1. Precision milling of blades

Generation of tool paths for machining blades using UG-CAM module, With the ball milling cutter ball center point as the reference, the ball milling cutter side tilt angle and front tilt angle are 90 °, 0 °, Helical milling strategy is often used for finishing curved blade surfaces, Extract the cross-section portion of the ball end milling cutter in contact with 1/2 of the blade, Analyzing the key contact position between the tool and the blade, the representative tool-workpiece contact arcs are mainly distributed in the AB, CD, EF and GH segments, as shown in Figure 2.
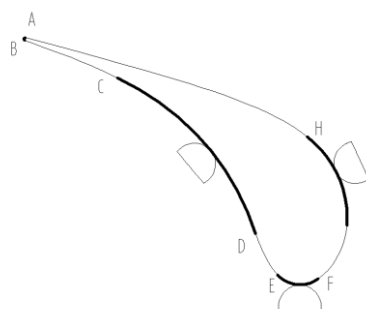

Figure 2. Cross section at blade-tool contact

Now based on the contact arcs of the cross-section, Let the radius of curvature of the blade profile be ρ , AB, EF, GH is "convex" and CD is "concave". Due to the extreme thinness of the AB section, "pitting" very easily occurs under milling forces, In the actual processing needs to be used to control the method of auxiliary offset thickening, so here will be the equivalent of the AB section radius of curvature of 3mm, the radius of curvature of each section is shown in Equation 1 - Equation 4.

$$\rho_{AB} \approx 3mm \tag{1}$$

$$\rho_{EF} \approx 8mm \tag{2}$$

$$\rho_{GH} \approx 25mm \tag{3}$$

$$\rho_{CD} \approx 55mm \tag{4}$$

(2) Geometric modeling and meshing

Leaf blades need to involve airways, leaf crowns, leaf bodies, and leaf roots, Among them, the main working part is the leaf body, to meet the relevant requirements, profiling milling method for machining, the machining method tool change position is complex, so you need to choose a reasonable tool geometry parameters, see table 1.

Table 1. Tool Geometry

radius (R/mm)	number of blades	helix angle($\beta/^{\circ}C$)	helix angle(L/mm)
10	4	30	8

$$\rho_{AB} \approx 3\text{mm} \qquad \rho_{EF} \approx 8\text{mm}$$

$$\rho_{GH} \approx 25mm \qquad \rho_{CD} \approx 55mm$$
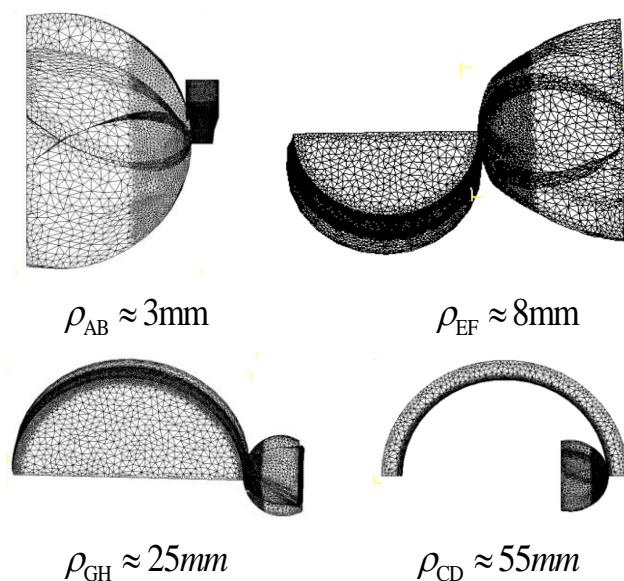
Figure 3. Meshing of profiles with different radii of curvature

Tool-workpiece modeling in UG, Export as .stl format file, Based on the Load Geometric Objects command in Deform, the tool-workpiece assembly is loaded, the tool is selected as a rigid body, and the workpiece is set to plasticity. To prevent calculation anomalies caused by distortions of cells during the milling of blades, Using adaptive meshing in Deform, For some regions with large changes in the gradient of the constant variable, To obtain more accurate data, the tool-workpiece critical contact portion is refined with a refinement ratio of 0.01, as shown in Figure 3.

(3) material eigenmodel

The TC4 titanium alloy, which has good mechanical and physical properties, is used for the simulation workpiece. Fine-grain carbide is used as the cutting tool material (e.g. YG6X), chip removal that is smooth, strong against wear, and resilient in finishing conditions, The main performance parameters of the tool and workpiece are shown in Table 2.

Table 2. Main performance parameters of ball end milling cutters and workpieces

Material Properties	WC	TC4 workpiece temperatures $/20°C \sim 650°C$
modulus of elasticity /GPa	650	110
densities $/(g / cm^3)$	16	4.5
heat conductivity $/(W/m \cdot K)$	59	5.44
Poisson's ratio	0.25	0.3
specific heat $/(J/g \cdot °C)$	0.96	0.56
durometerHRC	70	36

Due to the low modulus of elasticity of titanium alloy materials, poor machinability, and poor thermal conductivity, During the cutting process, the temperature of the workpiece material can reach 200-1000°C or even higher, therefore, it is extremely important to choose a reasonable material constitutive model. Through the research of many scholars [9-10], it is shown that the Johnson-Cook principal model is suitable for describing the high temperature, large strain, large strain rate is widely used, and can be a good secant of the material excision process, the JC principal model expression form is shown in Eq. 5:

$$\sigma = \left(A + B \varepsilon_P^n \right) \left[1 + C \ln \frac{\dot{\varepsilon}}{\dot{\varepsilon}_0} \right] \left[1 - \left(\frac{T - T_0}{T_{melt} - T_0} \right)^m \right] \tag{5}$$

Where: A is the initial yield stress; B is the material strain strengthening parameter; m is the hardening index; n is the material thermal softening index; ε is the equivalent plastic strain; $\dot{\varepsilon}$ is the equivalent plastic strain rate; $\dot{\varepsilon}_0$ is the material reference strain rate; T is the cutting temperature; T_m is the melting temperature; and Tr is the reference temperature. The values of the parameters were determined as shown in Table 3.

Table 3. Johnson-Cook model parameters

A(MPa)	B(MPa)	n	C	m
861	331	0.34	0.03	0.8

(4)friction model

When cutting metal, there is friction and plastic deformation between the front face of the tool and the chip, the back face, and the workpiece to generate cutting heat. Tool and chip simulation results can be affected by friction effects, At the same time, friction generates heat leading to high ambient temperatures and chemical reactions, resulting in tool wear. Therefore, the friction model is essential for the analysis of the cutting process, and the friction model for titanium alloys, as shown in Equation 6.

$$\tau_f = \begin{cases} \mu\sigma_n, \sigma_n < \tau_s & \text{(sliding-friction zone)} \\ \tau_s, \mu\sigma_n \geq \tau_s & \text{(bonding friction zone)} \end{cases} \tag{6}$$

Where: τ_f is the shear stress; τ_s is the ultimate shear stress; σ_n is the positive pressure; μ is the coefficient of sliding friction, set to 0.6 [11].

(5)Wear model

The amount of wear depends on the tool's face temperature, the positive pressure at the tool/chip and tool/work interface, and the relative sliding speed. Therefore, the Usui model is used in this paper. As shown in equation 7.

$$W = \int Cv_s\sigma_f \exp(-\lambda/T)dt \tag{7}$$

where v_s is the sliding speed of the tool relative to the workpiece; σ_f is a positive pressure, and T is the absolute temperature of the tool surface; C and λ are characteristic constants, depending on the tool and workpiece material. In this paper, C = 0.0000001, = 855 based on empirical values [12].

3. Design of Experimental Programs and Numerical Calculations

(1) Tool Wear-Temperature Data Calculation

The test parameters are spindle speed n=1900r/min, feed per tooth f_z=0.3mm/z, and milling depth a_p=0.45mm. Analyzing tool temperature and tool wear data with Deform, Through the post-processing interface output 500 steps of different curvature radius profile data milling model of tool wear and temperature change rule, as shown in Figure 4-5.
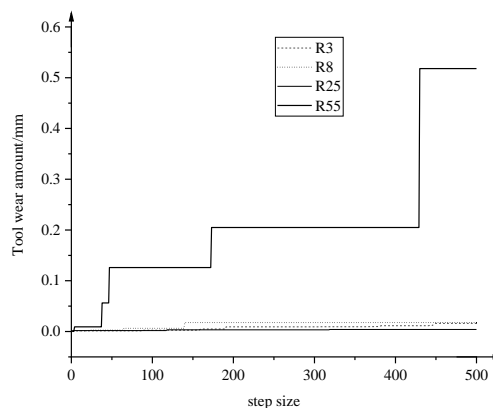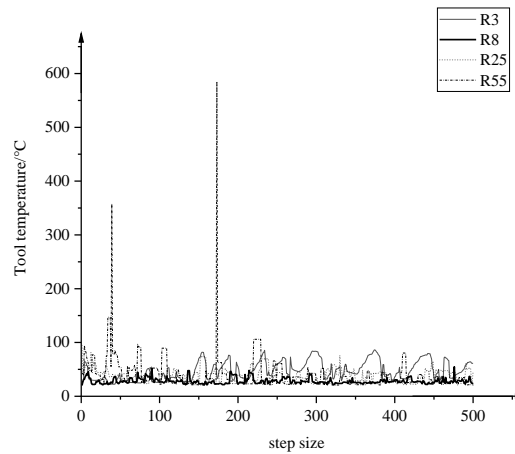

Figure 4. Variation of tool wear with different radii of curvature

Figure 5. Temperature variation of tools with different radii of curvature

From Figure 4 - Figure 5, When milling profiles with different radii of curvature in 500 steps, the tool temperature and tool wear are always greater for concave surfaces than for convex surfaces. Reason: The angle of incision for concave surface milling is smaller than that for straight line milling and decreases as the radius of curvature of the tool center trajectory curve increases. As a result, the cut angle interval (the difference between the cut-out angle and the cut-in angle, which indicates the size of the tool-chip contact range) of concave surface milling increases with the curvature, while concave surface milling causes the maximum undeformed chip thickness to increase, and increases with the curvature radius. The conclusions are opposite when milling convex surfaces and this paper focuses on the amount of tool wear on concave surfaces.

(2) Experimental program design and results

Table 4. BBD orthogonal test simulation and results

batch number	f_z (mm/z)	n (r/min)	a_p (mm)	W (mm)	Q ($cm^3 \cdot min^{-1}$)
1	0.3	800	0.1	0.00235	0.0192
2	0.1	3000	0.45	0.0218	0.108
3	0.5	1900	0.1	0.0072	0.076
4	0.3	3000	0.8	0.0339	0.576
5	0.5	800	0.45	0.0191	0.144
6	0.5	1900	0.8	0.178	0.608
7	0.3	1900	0.45	0.518	0.2052
8	0.1	1900	0.1	0.003	0.0152
9	0.3	1900	0.45	0.518	0.2052
10	0.3	1900	0.45	0.518	0.2052
11	0.1	1900	0.8	0.362	0.1216
12	0.1	800	0.45	0.0124	0.0288
13	0.3	3000	0.1	0.125	0.0953
14	0.3	800	0.8	0.105	0.1536
15	0.3	1900	0.45	0.518	0.2052
16	0.5	3000	0.45	0.226	0.54
17	0.3	1900	0.45	0.518	0.2052

Using Design-Expert data analysis software, BBD in RSM was selected to obtain a representative orthogonal test combination scheme as shown in Table 4.

Table 4 Minimum wear of 0.00235mm was obtained in all program groups, and the maximum reached 0.518mm beyond the range of the tool wear, Accelerated reduction of tool life, very easily leads to substandard blade machining quality, The material removal rate is very low, resulting in low machining efficiency and high machining cost, so the process parameters need to be optimized to improve tool life and blade quality is the current need to solve the problem.

4. Optimization of Process Parameters

(1) Modeling multivariate nonlinear regression

Depending on the purpose of the research question, In this paper, we use a ternary quadratic regression equation and set the dependent variables to be the amount of tool wear and the amount of material removed, The independent variables that are statistically related to this dependent variable are selected as process parameters and the general form of the equation is:

$$Y = \beta + \sum_{i=1}^{m} \beta_i x_i + \sum_{i \leq j}^{m} \beta_{ij} x_i x_j + \sum \beta_{ii} x_i^2 + \xi \tag{8}$$

where Y is the target estimate; β is the coefficient estimate; β_i is the linear coefficient; β_{ij} is the quadratic term coefficient; β_{ii} is the interaction term coefficient; α is the test error; and x_i is the cutting parameter code.

(2) Establishing empirical equations

By processing the experimental data, the model was analyzed by ANOVA and fitted to obtain an empirical model for tool wear W as:

$$\begin{aligned} W &= 0.033905 + 1.00104 \times f_z - 0.000279 \times n \\ &+ 0.22193 \times a_p - 0.000665 \times f_z \times n + 0.908571 \times f_z \times a_p \\ &+ 0.000054 \times n \times a_p + 1.04156 \times f_z^2 + 0.0000001124 \times n^2 \\ &- 0.175204 \times a_p^2 \end{aligned} \tag{9}$$

(3) Determination of optimization variables and objective function

The simultaneous optimization multi-objective proposed in this paper is smaller tool wear and, a higher material removal rate with mathematical description and constraints:

$$\begin{cases} F_1 = \min W(f_z, n, a_p) \\ F_2 = \max Q(f_z, n, a_p) \\ 0.1mm/z \leq f_z \leq 0.5mm/z \\ 800r/\min \leq n \leq 3000r/\min \\ 0.1mm \leq a_p \leq 0.8mm \end{cases} \tag{10}$$

The material removal rate Q is calculated as:

$$Q = nf_z a_e a_p z / 1000 \tag{11}$$

(4) Optimization results of machining process parameters

The basic idea of a multi-objective optimization algorithm is: First, an initial population of size N is randomly generated, After non-dominated sorting, the first population of offspring (population) is obtained by the three basic operations of genetic algorithms: selection, hybridization, and mutation; Second, starting with the second generation, the parent group (population) is merged with the offspring population, Perform fast non-dominated sorting, Crowding is also calculated for individuals in each non-dominated layer, Selection of suitable individuals to form a new parent population based on non-dominance relationships and crowding of individuals, Finally, new offspring populations are generated by the basic operations of the genetic algorithm.

A multi-objective optimization technique can be used to swiftly produce non-dominated, preferred solutions. Coding techniques, initial value assignment, fitness function with quick non-dominated sorting, and congestion calculation are all used in multi-objective optimization algorithms to obtain the Pareto optimal solution set. Its main flow is shown in Figure 6.
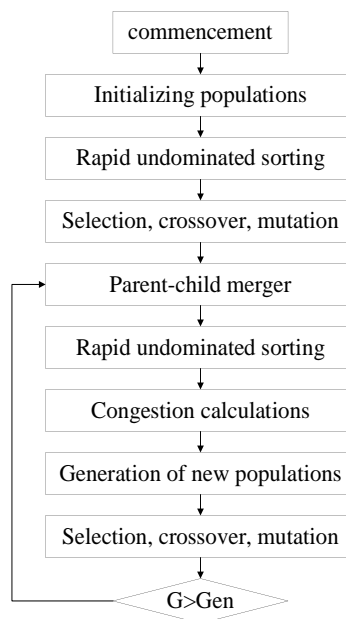
Figutr 6. Flowchart of multi-objective optimization algorithm

Set the initialization population to 50 and the maximum number of iterations to 300, The crossover ratio is 0.08 and the probability of crossover difference is 0.05, Obtaining the Pareto optimal solution set. To facilitate the selection and comparison of process parameters during actual machining, four groups of optimized process parameters are taken randomly, as shown in Table 5.

Table 5. Pareto optimal solution set

serial number	f_z (mm/z)	n (r/min)	a_p (mm)	w (mm)	Q ($cm^3 \cdot min^{-1}$)
1	0.36	2060	0.44	0.023	1.2222
2	0.46	1900	0.60	0.027	1.4945
3	0.49	1990	0.70	0.074	1.7464
4	0.475	2150	0.30	0.022	1.7566

From the table, it can be seen that to control the amount of tool wear you need to focus on controlling the size of the depth of cut, Maximum tool wear of 0.0735 mm in 4 sets of optimized machining parameters, and Meet the amount of tool wear within the range.

From Figure 7, it can be seen that the overall tool wear and material removal rate obtained by the group of 17 multi-objective optimization algorithms is smaller than that obtained by the group of BBD orthogonal test schemes, To verify the effect after optimization, the objective function values and process parameter groups before and after optimization of 1 group in the figure were arbitrarily selected for comparison, and the results are shown in Table 6.
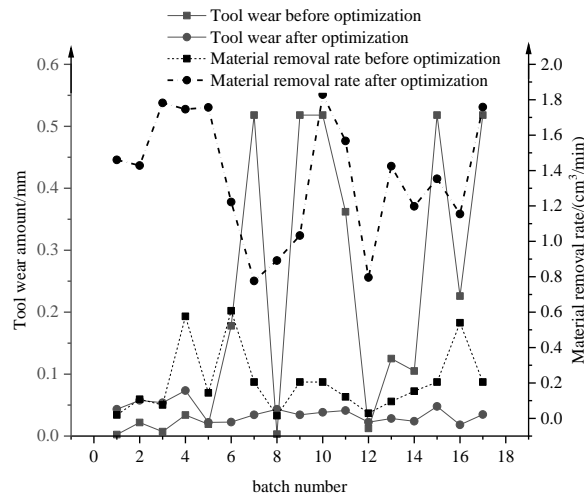

Figure 7. Comparison of tool wear and material removal rate before and after optimization

Table 6. Rate of change before and after optimization

	f_z (mm/z)	n (r/min)	a_p (mm)	w (mm)	Q ($cm^3 \cdot min^{-1}$)
pre-optimization	0.30	1900	0.450	0.158	0.2052
post-optimization	0.45	1899	0.592	0.043	1.4605
variation difference				0.115	-1.2553

In Table 6, the optimized feed per tooth, spindle speed, and milling depth are increased. Tool wear was reduced by 0.115mm and material removal increased by -1.2553 $cm^3 \cdot min^{-1}$.

5. Conclusion

In this paper, DEFORM-3D is utilized as the main tool for simulating the tool wear process and calculating the process parameters were optimized using a multi-objective optimization algorithm and the conclusions are as follows:

A three-dimensional thermodynamically coupled rigid-plastic finite element model of metal cutting was established to obtain tool temperature and tool wear data to investigate, It is verified that the maximum temperature and wear of tools on convex surfaces are less than those on concave surfaces, A study related to the acquisition of data on the amount of wear of comparable tools available.

Study of a tool wear control program that synthesizes high material removal rates, According to the parameters to be set in the CAM software and the actual machining situation in the factory. Adding high material removal rates to tool wear influencing factors, An orthogonal test scheme was used to

simulate the acquisition of the dataset, combined with a multi-objective optimization algorithm for the optimization of the process parameters, to obtain practically usable process parameters for high material removal rate and low tool wear.

The study focuses on developing a tool wear control program that can achieve high material removal rates based on the parameters set in the CAM software and the actual machining conditions in the factory. By incorporating high material removal rates as one of the influencing factors for tool wear, we obtained a dataset through simulation using an orthogonal test scheme. We then optimized the process parameters using multi-objective optimization algorithms to obtain practically usable parameters that ensure both high material removal rates and low tool wear.

Acknowledgments

References

[1] LI X, YU J H, ZHAO P. Research Status of Machining Deformation Control Method and Technology of Aeroengine Blade[J].Aeronautical Manufacturing Technology,2016(21):41-49+62.

[2] ZHENG Min-li,WU Di,YANG Lin,MA Hui .Research on Cutting Force Prediction for Corner Machined with Ball End Mill [J]. Machinery Design & Manufacture, 2017(04):85-88.DOI:10.19356/j.cnki.1001-3997.2017.04.022.

[3] WANG Xiao- chun, HU Ying- ning, SU Jia- qiang .Study on relationship between tool path of curvature and milling force with micro- end mill [J]. Machinery Design & Manufacture, 2008(10):205-207.

[4] Ju Yang.Research on cutting temperature and tool wear for machining complex surface of titanium alloy[D]. Nanjing University of Science & Technology. 2020.DOI:10.27241/d.cnki.gnjgu.2020.001539.

[5] Xiaoliang Liang. Effects of tool wear state on the Machined Surface Integrity of Titanium Alloy Ti-6Al-4V[D]. SHANDONG UNIVERSITY, 2021.DOI:10.27272/d.cnki.gshdu.2021.000069.

[6] Liu Y , Wen X , Niaoqing H U . SURROGATE DATA TEST FOR THE LINEAR NON-GAUSSIAN TIME SERIES WITH NON-MINIMUM PHASE[J]. Acta Physica Sinica, 2001, 50(4).

[7] Senthil Kumar A , Raja Durai A , Sornakumar T . The effect of tool wear on tool life of alumina-based ceramic cutting tools while machining hardened martensitic stainless steel[J]. JOURNAL OF MATERIALS PROCESSING TECHNOLOGY, 2006.

[8] Jawahir I S , Ghosh R , Fang X D , et al. An investigation of the effects of chip flow on tool-wear in machining with complex grooved tools[J]. Wear, 1995, 184(2):145-154.

[9] Wang B, Liu Z . Shear localization sensitivity analysis for Johnson-Cook constitutive parameters on serrated chips in high-speed machining of Ti6Al4V[J]. Simulation Modelling Practice & Theory, 2015, 55:63-76.

[10] YANG Yang,LI Jin-liang ,ZHOU Lianga.Research on Cutting Thermal Modeling and Simulation of Turning AISI 1045[J]. Modular Machine Tool & Automatic Manufacturing Technique. 2018(05):34-36.

[11] Zhitao Tang. Residual Stresses and Deformations of Aerospace Aluminum Alloy in Machining[D]. SHANDONG UNIVERSITY, 2008.

[12] YanHong XaiJuchen. Numerical Simulation of Fine Turning for H13 Hardened Die Steel[J]. China Mechanical Engineering, 2005(11):985-989.

[13] Feng Shi,Hui Wang,Lei Yu. MATLAB Intelligent Algorithms 30 Case Studies[M].Beijing: Beijing University of Aeronautics and Astronautics Press,2011.

[14] Jingmin Sun,Yingchun Liang.Mechanical Optimization. 5th edition[M]. Machinery Industry Press,2021.